AMERICAN UNIVERSITY OF BEIRUT

PERFORMANCE EVALUATION OF THE
DISPLACEMENT VENTILATION COMBINED WITH
EVAPORATIVE COOLED CEILING FOR A TYPICAL
OFFICE IN BEIRUT

by
MANAR FAWZI YOUNIS

A thesis
submitted in partial fulfillment of the requirements
for the degree of Master of Applied Energy
to the Department of Mechanical Engineering
of the Faculty of Engineering and Architecture
at the American University of Beirut

Beirut, Lebanon
August 2015

AMERICAN UNIVERSITY OF BEIRUT

PERFORMANCE EVALUATION OF THE DISPLACEMENT VENTILATION COMBINED WITH EVAPORATIVE COOLED CEILING FOR A TYPICAL OFFICE IN BEIRUT

by
MANAR FAWZI YOUNIS

Approved by:

_____   Advisor
Prof. Kamel Abou Ghali, PhD, Professor
Department of Mechanical Engineering

_____   Co-Advisor
Prof. Nesreen Ghaddar PhD, Professor
Department of Mechanical Engineering

_____   Member of Committee
Prof. Mohammad Ahmad, PhD, Professor
Department of Chemical and Petroleum Engineering

Date of thesis defense: August, 28, 2015

AMERICAN UNIVERSITY OF BEIRUT

THESIS, DISSERTATION, PROJECT RELEASE FORM

Student Name: __Younis_____ __Manar_____ __Fawzi_____
                       Last   First   Middle

☑ Master's Thesis   ○ Master's Project   ○ Doctoral Dissertation

☒ I authorize the American University of Beirut to: (a) reproduce hard or electronic copies of my thesis, dissertation, or project; (b) include such copies in the archives and digital repositories of the University; and (c) make freely available such copies to third parties for research or educational purposes.

☐ I authorize the American University of Beirut, **three years after the date of submitting my thesis, dissertation, or project,** to: (a) reproduce hard or electronic copies of it; (b) include such copies in the archives and digital repositories of the University; and (c) make freely available such copies to third parties for research or educational purposes.

__Manar_____   __22/9/2015_____

Signature   Date

ACKNOWLEDGMENTS

AN ABSTRACT OF THE THESIS OF

Manar Fawzi Younis   for   Master of Engineering
                              Major: Applied Energy

Title: Performance Evaluation of the Displacement Ventilation Combined with Evaporative Cooled Ceiling for a Typical Office in Beirut

Displacement ventilation (DV) system combined with a novel evaporative cooled ceiling (ECC), Maisotsenko cycle (M-cycle), is a passive technique proposed to enhance the load removal in spaces beyond the conventional DV limit of 40 W/m^2. In this study, predictive mathematical models of the conditioned space and the evaporative cooled ceiling were developed to study the performance of the integrated system. The integrated DV/ECC mathematical model was validated experimentally showing good prediction of ceiling temperature and room conditions at different space loads.

A parametric study was done in order to study the limitations of the system, where it showed better efficiency at higher supply flow rates and lower supply air relative humidity. The validated DV/ECC system model was applied for a typical office in the city of Beirut, where a control strategy of increasing the supply flow rate was implemented to the DV system, while maintaining a stratification height of 1.5 m. The integrated system is operated only when the DV system cannot attain comfort in the space anymore. The load removal by the DV/ECC reached 50 W/m^2, exceeding by 20% the maximum limit of 40 W/m^2 of the unaided DV system. Moreover, the proposed DV/ECC system resulted in 36.2 % reduction in electric energy consumption in the summer months when compared with a conventional DV and chilled ceiling system.

CONTENTS

NOMENCLATURE

A	Area (m)
CC	chilled ceiling
COP	coefficient of performance
C_p	specific heat (J/kg·K)
DV	displacement ventilation
ECC	evaporative cooled ceiling
h_c	convective heat transfer coefficient (W/m^2·K)
$h_{cv,f}$	heat transfer coefficient at the floor level (W/m^2·K)
h_{fg}	latent heat of evaporation (J/kg)
h_m	mass transfer coefficient (m/s)
h_r	linearized radiative heat transfer coefficient (W/m^2·K)
H	enthalpy in J/kg
IAQ	indoor air quality
k	thermal conductivity (W/m·K)
k_{e1}	effective thermal conductivity of the heat transfer plate (W/m·K)
k_{e2}	effective thermal conductivity of the ceiling (W/m·K)
M	flow rate from wall plumes, heat sources, and supply (kg/s)
MRT	mean radiant temperature
PMV	predictive mean vote

Q	load (W/m^2)
Qs	supply flow rate (m^3/s)
$\dot{q}$	radiative heat load (W/m^2)
T	temperature (°C)
Ts	supply temperature (°C)
ω	humidity ratio (kg/kg)
ω^*	humidity ratio of saturated air (kg/kg)
x	axial coordinate of the channel in the flow direction (m)
Z	elevation above floor level (m)

Greek Symbols

Φ	heat source strength (W)
δ	channel height (m)
δ_{e1}	effective thickness of the heat transfer plate (m)
δ_{e2}	effective thickness of the ceiling (m)
ρ	density (kg/m^3)
v	air velocity (m/s)

Subscripts

c	ceiling
d	dry channel
p	heat transfer plate
pl	plume

r	room
$s_1,\ s_2$	water absorbing sheets
w	wet channel or room wall

ILLUSTRATIONS

TABLES

CHAPTER I

COMBINED DISPLACEMENT VENTILATION NOVEL EVAPORATIVE COOLED CEILING SYSTEM

A. Introduction

Thermal comfort and indoor air quality are considered to be important factors for occupants in spaces. To achieve comfort and good air quality in indoor spaces, conventional cooling systems consume energy [1, 2]. Therefore, alternative cooling and ventilation systems are sought to supply occupants with a healthy and comfortable indoor space, but with better performance [3, 4].

One of the ventilation systems that is known for its effectiveness in providing high indoor air quality and is widely used in office buildings is the displacement ventilation (DV) system [5]. In DV systems, indoor air quality (IAQ) is achieved through supplying 100% fresh air [6], but it is constrained by a supply air temperature not less than 18°C to maintain thermal comfort and a supply air velocity not greater than 0.2 m/s to avoid any thermal draft in the occupied zone [7]. These two constraints, relatively high supply air temperature and low air velocity, not only limit the application of the DV system to low cooling loads of less than 40 W/m^2 [8, 9] but also decrease the system's energy efficiency in hot and humid environments. This major limitation has encouraged researchers to look for other alternatives to increase the load removal in spaces without compromising indoor air quality and thermal comfort. Therefore, chilled ceiling systems were introduced in order to increase the cooling load capacity of the DV system [10]. Part of the sensible load is removed by the chilled ceiling (CC) [11, 12] while the other part is removed by the DV system in addition to the removal of space

latent load [13]. However, the integration of a CC with a DV system will result in added energy cost due to the chilled ceiling and the costs associated with the constraint on supply humidity to prevent condensation on the ceiling if exhaust air dew point temperature is higher than the ceiling temperature. Thus, researchers considered solar-assisted solid desiccant dehumidification technology to reduce supply air relative humidity of the DV system [14, 15, 16]. However, in spite of the good efficiency of such systems, they seem to have a high installation and maintenance cost [14].

A suggested solution to overcome issues related to limited load removal is the use of a dew point evaporative cooled ceiling that works based on the principle of the Maisotsenko cycle (M-Cycle) [17,18]. The evaporative cooled ceiling takes the warm air from the space and then cools it down due to water evaporation after absorbing the heat from it. This will result in having an air temperature that approaches the dew point temperature. Then, air will be heated due to the heat exchanged with the ceiling that will cool the ceiling and consequently the space without added energy consumption to the DV system [17, 18, 19]. Miyazaki et al. [19] performed a study to develop a passive cooling device represented by a dew point evaporative cooler integrated with the ceiling panel and a solar chimney, where air from the room is taken as inlet to the evaporative cooler. The cooling performance was simulated to show that 40-50 W/m^2 of radiative cooling load can be removed without a significant increase in the ceiling temperature.

The purpose of this study is to develop a cooling system that effectively increases the cooling load capacity of the displacement ventilation system to a limit beyond 40 W/m^2 [20, 21, 22] by enhancing its performance through a dew point evaporative ceiling cooler (ECC). A mathematical model is developed to predict the energy performance of the combined DV/ECC system. The model is validated

2

experimentally by comparing predicted and experimentally measured ceiling and room temperatures. The model limitations are assessed for satisfying both thermal comfort and indoor air quality at specified operating conditions. Finally, a comparison of the electric consumption of the proposed combined system and a typical CC/DV system will be conducted for an office in Beirut.

B. System Description

Figure 1 presents a schematic of the (a) combined DV/ECC air conditioning system and (b) ECC process on psychometric chart. The system incorporates the novel evaporative cooled ceiling incorporating an M-cycle applied to a hot and humid climate for space cooling. In DV system, fresh air is allowed to enter the chiller in order to cool it below its dew point temperature and control its humidity and then it will be introduced to a reheating coil in order to increase its temperature to the desired DV supply value. Cool supply air at flow rate (Qs) enters the space at floor level (1) at temperature (Ts) and spreads through the space and then rises as it warms due to heat exchange with heat sources (e.g., occupants, computers, lights, etc.). Warm air has lower density than the cool air, so an upward convective flow will be created due to buoyancy. As a result, the lower occupied zone will contain the fresh cool air coming from the supply, while the air carrying contaminants and heat in the space rises to the ceiling level [15] dividing the space into two zones separated by the stratification height, which is the level at which the rate of air entrained by the buoyancy plumes equals the supply flow rate [21]. The warm air near the ceiling will represent the supply air entering the evaporative cooled ceiling at (2) as shown in Fig. 1.

3

The dew point ECC consists of two channels: a wet and a dry one separated by a plate of high conductivity to enhance heat exchange. Warm air from the upper zone of the space is directed to enter the ceiling setup, where it first flows in the dry channel and then is diverted to the wet channel at (3) (Fig. 1). Because of the counter flow, the air in the dry channel will be cooled without adding humidity to it (follow psychrometric process in Fig. 1b), while the temperature of the air in the wet channel increases and gains moisture to evaporatively cool the ceiling and then the air leaves the ECC at point (4). This will result in enhancing the cooling performance of the DV system without additional energy consumption.
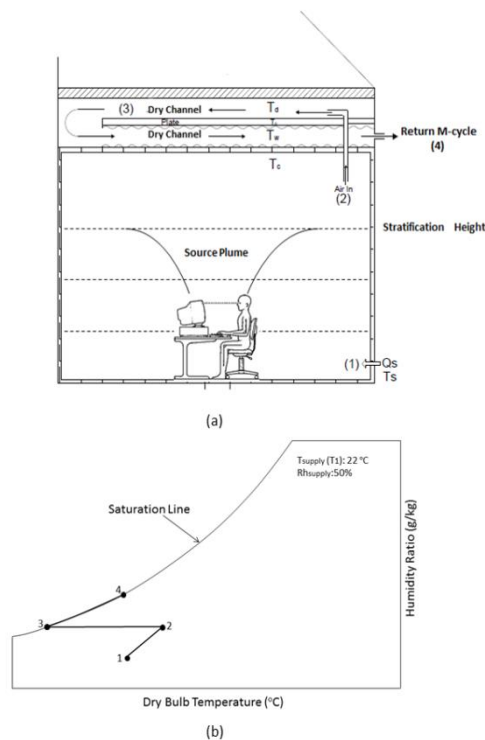

Figure 1: Schematic of the combined air conditioning system

CHAPTER II

MATHEMATICAL MODELS AND SOLUTION MEHODOLOGY

A. Displacement Ventilation Space Model

The space model of Ayoub et al. [21] was adopted to calculate the different space temperatures. The space is divided into four adjacent horizontal air layers with adjacent wall layers (see Fig.1). Each layer is represented by a uniform temperature $T(i)$ where i corresponds to the air layer index (i =1 to 4) . Each layer interacts with side wall segments. The one-dimensional heat conduction equation for a multi-layered discretized wall is used to calculate the wall temperatures, taking into consideration the external and internal boundary conditions that account for ambient conditions, internal and external heat sources and different envelope materials. The ECC ceiling temperature T_c is constant and uniform since it is highly conductive material. The internal lumped air energy balance at each horizontal layer is also done, in order to get the air temperatures at different elevations, assuming air movement in the vertical direction. At each air layer, wall and heat source plumes are considered, which affect the internal air temperatures. The energy associated with the source plume is calculated from the model of Mundt [22] while the energy associated with the wall plumes is calculated from the work of Jaluria [23].

The flow rates resulting from walls and heat sources are denoted by $M_{w(j,k)}$ and $M_{p(l,k)}$ respectively. The net circulated mass M_{cir} at each boundary (interface surface

between two adjacent air layers i and $i+1$) will be calculated. The enclosure mass balance equation is given by

$$M_{cir,k} = M_s - \sum_{l=1}^{r} M_{pl,(l,k)} - \sum_{j=1}^{4} M_{w,(j,k)} \qquad (1)$$

In the above equation 7, k refers to the interface level between the consecutive air layers ($k=1$, 2 or 3 for a space divided into four layers) and r is the number of heat sources in the first air layer. If the circulation mass is positive, then the circulated mass is moving upward, while if it is negative then the circulated mass is moving downward. The determination of this circulated mass is very important because the stratification height is defined at the level when the circulated mass is zero [21].

The energy balance is then written for each horizontal air layer and for each wall segment [18]. The first air layer energy balance is given by

$$\sum_{l=1}^{r} \Phi_{(l,1)} + \sum_{i=1}^{4} h_{cv,(i,1)} A_{w,(i,1)} (T_{w,(i,1)} - T_{a,(1)}) + h_{cv,f} (T_f - T_{a,(1)}) +$$
$$M_s H_s = \sum_{j=1}^{r} M_{pl,(j,1)} H_{pl,(j,1)} + \sum_{i=1}^{4} M_{w,(i,1)} H_{w,(i,1)} + M_{cir,1} H_{cir,1} \qquad (2)$$

where Φ is the heat source flux, H is the enthalpy in J/kg, $h_{cv,f}$ is the convective heat transfer from the floor level. For the left hand side of Equation (2), the first term is the summation of the heat fluxes in the first layer, the second and third terms are heat convection from the walls and the floor, and the fourth term is the enthalpy of the supply air. For the right hand side of Equation (2), the first and second terms are the enthalpies of the heat sources and wall plumes and the third term is the enthalpy of the circulated mass at the boundary. The energy balance equations on the two intermediate

6

layers and the upper layer were similarly derived by Ayoub et al. [21] and will not be repeated here.

Modeling of heat sources plumes in presence of temperature gradients will follow the expressions given by Mundt [22]. The plume flow rate Q_{pl} at elevation Z above the floor through depends on the plume source strength, Φ, and vertical temperature gradient, dT_a/dZ, can be calculated by the following steps [22]:

$$Q_{pl} = 0.00238\Phi^{3/4}(\frac{dT_a}{dZ})^{-5/8}B_1 \tag{3a}$$

$$A_1 = 2.86(Z - Z_p)(\frac{dT_a}{dZ})^{3/8}\Phi^{-1/4} \tag{3b}$$

$$B_1 = 0.004 + 0.039A_1 + 0.38A_1^2 - 0.062A_1^3 \tag{3c}$$

where Z_p is the source height from the ground level.

The integrated wall and plumes mathematical models are used to calculate the stratification height and the vertical temperature gradient along the different air layers. To solve the energy balance equations of the enclosure air layers, the values of the air flow rates passing from one layer to the other due to the generated plumes from the heat sources and the walls are calculated from the plume equation for the sources and using the wall plume model [23].

B. Evaporative Cooled Ceiling Mathematical Model

The developed model of Miyazaki et al. [19] was adopted for the evaporative cooled ceiling to determine the load removal based on the space conditions and ceiling temperature influenced by the air flow in the dry and wet channels. The ECC system model is a one dimensional steady state model that considers variation in temperature

and humidity of air within the two-pass channel. The assumptions made were that the temperature gradients along the heat transfer plate, the water sheets and the ceiling were neglected and the heat gain through the roof was also neglected, since the top side of the dry channel was assumed insulated.

The sensible heat balance of air in the dry channel where the temperature of air is   lowered is represented in the following equation:

$$\rho C_{pd} v \delta \frac{dT_d}{dx} = h_d (T_p - T_d) \tag{4}$$

Where x is the axial coordinate of the channel in the flow direction, ρ represents the air density in the channel, C_{pd} represents the heat capacity of the dry air, v is the velocity of air, δ is the height of the channel, and h_d represents the convective heat transfer coefficient in the dry channel. The heat transfer to the air flow in the dry channel is equal to the conducted heat from channel plate to the flowing air, where Air temperature in the dry channel is denoted by T_d while the plate temperature is denoted by T_p.

The sensible heat balance of air in the wet channel is given by

$$\rho C_{pw} v \delta \frac{dT_w}{dx} = h_{s1} (T_{s1} - T_w) + h_{s2} (T_{s2} - T_w) \tag{5}$$

The net heat exchange with the two sides of the wet channel is equal to the net convective heat flow in the wet channel, where C_{pw} represents the heat capacity of the wet air, and h_{s1} and h_{s2} represent the convective heat transfer coefficients of the two absorbing sheets in the wet channel. Temperature of the air in the wet channel is denoted by T_w while the temperatures of the upper and the lower water absorbing sheets of the wet channel are denoted by T_{s1} and T_{s2} respectively. The convective heat transfer

coefficients h_d, h_{s1} and h_{s2} were calculated from the Nusselt number of a developed flow in rectangular shape channels [19].

The mass balance of the wet channel where the net convective flow of moisture is equal to the moisture exchange with the two water sheets of the wet channel is given by

$$\frac{dw}{dx} = \frac{h_{m1} + h_{m2}}{v\delta}(w_w^* - w_w)$$ (6)

w_w^* represents, at temperature T_w, the humidity ratio of saturated air, w_w is the humidity ratio of air in the wet channel, h_{m1} and h_{m2} represent the mass transfer coefficients in the wet channel and found using the Lewis number.

The energy balance of the heat transfer plate is given by

$$h_d(T_d - T_p) + \frac{k_{e1}}{\delta_{e1}}(T_{s1} - T_p) = 0$$ (7)

where k_{e1} and δ_{e1} represent the effective thermal conductivity and the effective thickness of the heat transfer plate respectively. In Equation (4), the heat transfer between the plate and the dry channel is equal to the net conductive heat between the plate and upper water sheet of the wet channel.

The energy balance of the upper water sheet is formulated such that the net heat exchange of the upper sheet with the plate and the flowing air in addition to the latent heat are taken into consideration. Similarly, for the lower water sheet, the net heat exchange of the water sheet with the ceiling and the flowing air in addition to the latent heat are also considered. The energy equations are given for the upper and lower water sheets of the wet channel, respectively as follows:

9

$$\frac{k_{e1}}{\delta_{e1}}(T_p - T_{s1}) + h_{s1}(T_w - T_{s1}) + \rho h_{m1} h_{fg}(w_w - w_w^*) = 0 \tag{8}$$

$$\frac{k_{e2}}{\delta_{e2}}(T_c - T_{s2}) + h_{s2}(T_w - T_{s2}) + \rho h_{m2} h_{fg}(w_w - w_w^*) = 0 \tag{9}$$

where k_{e2} and δ_{e2} represent the effective ceiling thermal conductivity and thickness respectively, T_{s1} and T_{s2} are the temperatures of the upper and the lower water absorbing sheets of the wet channel as defined earlier, T_w is the air temperature in the wet channel, w_w^* represents the, the humidity ratio of saturated air at T_w, w_w is the humidity ratio of air in the wet channel, h_{m1} and h_{m2} are the mass transfer coefficients in the wet channel, and h_{fg} is the latent heat of evaporation

Finally, the energy balance corresponding to the ceiling, where the ceiling heat exchange with the lower water sheet of the wet channel, convection with the air inside the room near the ceiling and radiation with the space are taken into consideration and the balance is given by

$$\frac{k_{e2}}{\delta_{e2}}(T_{s2} - T_c) + h_c(T_r - T_c) + \dot{q} = 0 \tag{10}$$

Where T_c represents the ceiling temperature, h_c represents the convective heat transfer coefficient between the air near the ceiling and the ceiling surface, T_r represents the temperature of the air near the ceiling, and $\dot{q}$ represents the radiative heat load from the space.

C. Solution Methodology

Mathematical models for the different system components are developed and integrated to solve for the system variables and predict its performance as shown in the flowchart in Fig. 2. The inputs for the integrated system are represented by the outdoor weather conditions, supply air conditions, internal loads, envelope properties and space and ceiling setup geometry and physical dimensions.

The considered space is divided into n layers in the vertical direction [20, 21]. The temperature profile in the space in addition to the walls and ceiling temperatures are first assumed. Then, the DV space thermal model solves the air layers energy balance equations, taking into account the thermal plumes from internal heat sources as well as wall plumes, to obtain the temperature profile and gradient as well as the stratification height in order for the evaporative cooled ceiling model to update the ceiling temperature. The previous steps are repeated until convergence, set to 10^{-6}, is reached. Once convergence is reached, the temperature distribution in the space is determined as well as the energy performance of the system. The coupled mass and energy equations are discretized into algebraic equations using the finite volume method.
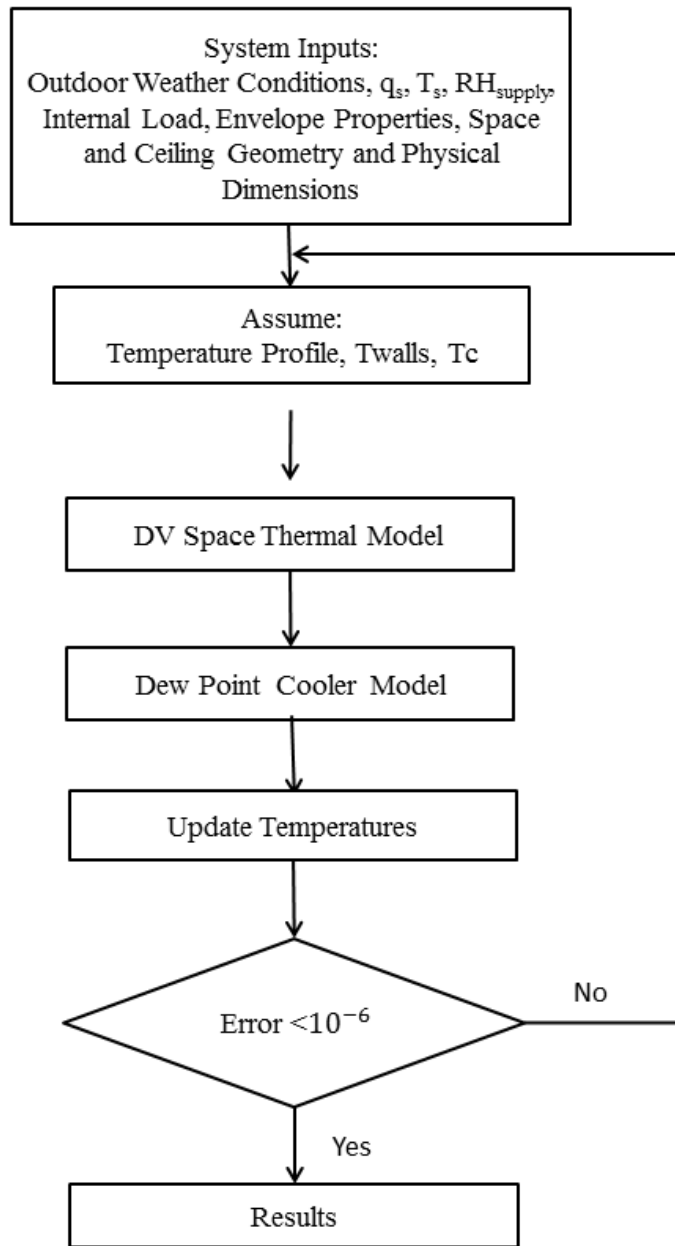
Figure 2: Sequence of numerical solution flowchart

CHAPTER III

MODEL VALIDATION

A. Experimental Setup of the Integrated DV/ECC System

The experimental validation was done by using a climatic chamber equipped with displacement ventilation system coupled with an evaporative cooled ceiling system as shown in Fig. 3(a). Room air temperatures at different levels and at the inlet of the ceiling setup were measured using HX94AC rod sensors with an accuracy of ±0.5 °C in temperature connected to a data logger OM-DAQPRO-3500 to record data every minute. The east, west, north and south walls of the chamber as well as the ceiling temperatures were measured using K-type thermocouples with an accuracy of ±0.5 °C in temperature. The supply and exhaust air temperatures and relative humidity were measured using OM-EL-USB-2 sensors with an accuracy of ±0.5 °C in temperature and ±3 % in relative. The supply air velocity was measured by BK PRECISION 731A velocity meter with an accuracy of $\pm3\%$ in velocity readings. The room walls have vapour barriers to prevent any moisture migration from the walls so that water vapour generation is controlled by supply air and internal sources.

The chamber's conditioned space by the integrated DV/ECC system has a total floor area of 5.56 m^2 and is 2.8 m high, where all walls were insulated by Styrofoam boards as shown in Fig. 3(b). The supply grill is located on the east wall supplying air at a flow rate of 0.118 m^3/s $\pm$ 0.00354 m^3/s, temperature of 22 °C $\pm$ 0.5°C and relative humidity of 50 % $\pm$ 3%. The air conditioning system is a controlled displacement

13

ventilation system, associated with an external fan coil unit to supply fresh air. Air

passes through a chiller of 6-kW capacity outside the room and is then introduced into a

heating coil to control its temperature and humidity. The load to be removed by the

integrated system was due to internal heat sources represented by non-moving seated

occupants, simulated by heated cylinders of 0.3 m diameter and 1.2 m height, each
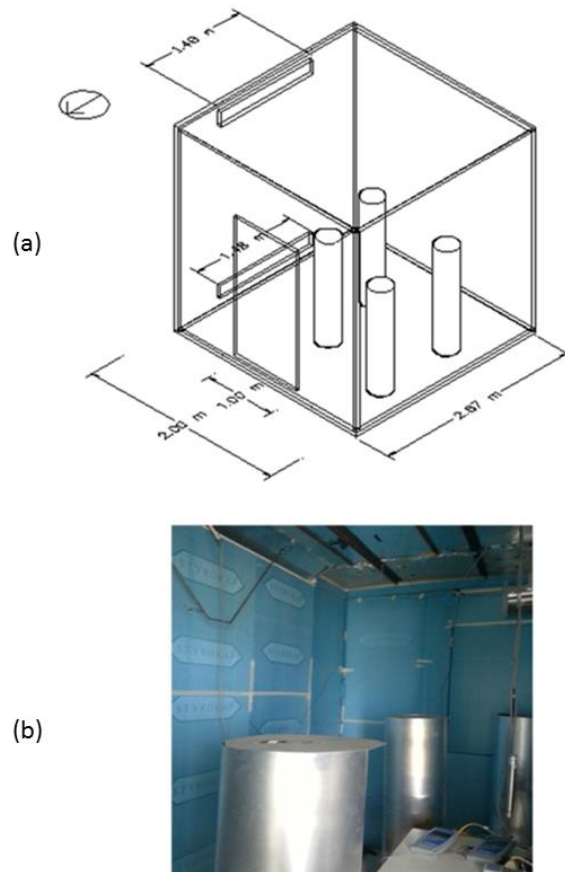
having a heat load of 100 W [24].

(a)

(b)

Figure 2: Plots of (a) schematic of the experimental setup and (b) photo of the

experimental room

14

As for the dew point cooler, it was made of commercial galvanized steel. The upper and lower sides of the wet channel in the ceiling setup were covered with a pure cotton wet fabric of high wicking capacity and fixed by means of a mesh to keep it in place. The cotton fabric at the two sides was associated with a thin perforated hose as shown in Fig. 4, and connected to two manual pumps to ensure even distribution of water along the channel. Each pump supplied one side of the wet channel, and water was maintained from a tank outside the room. The dry channel was insulated by fiberglass to avoid heat exchange along its sides where each channel is 3 cm high, and the setup covered all the ceiling area of 5.56 m^2. Note that the total height of the two pass channel is 6 cm which has a minor effect on the floor to ceiling height. In addition, the ECC installation does not constitute an added heavy load on the ceiling structure since it is made of thin light metal sheets with air as the running fluid. In order to control the system operation, air in the space can be diverted to the evaporative cooled ceiling setup by the means of a hinge as shown in Fig. 3(b). When the hinge is closed, air enters the ceiling setup and then is exhausted to the atmosphere so that the integrated system is operated, while when the hinge is opened, air directly leaves the space through the exhaust grill without entering the ECC setup so that only the DV system will be operated.
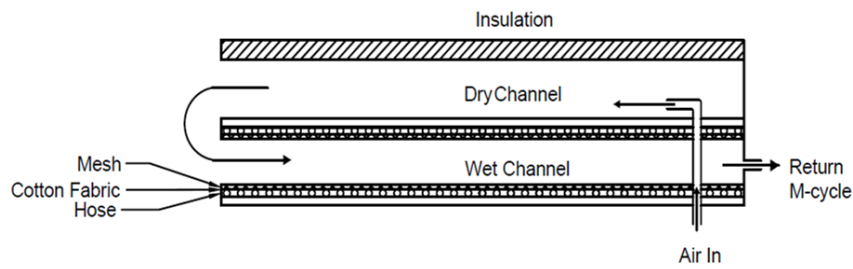
Figure 3: Schematic of the ECC channels

Three sets of experiments were done, each at a specified internal load namely 200, 300 and 400 W. Each set of experiments was done for two systems: first by operating the DV system alone, and then by operating the integrated ECC/DV system. In order to reach quasi-steady conditions, the system was operated for 4 hours, where the temperature variations were monitored until they stopped varying. The temperatures obtained experimentally will be compared to values predicted by the integrated system simulation model, where the inputs of the experimental setup represented by the supply air conditions and the different internal loads were taken the same when simulating the integrated model. Also, the Predicted Mean Vote (PMV)-index value is obtained, which is a representation of the thermal comfort from a scale between -3 (cold) to +3 (hot) with a comfort range of $-0.5 \leq PMV \leq +0.5$ [25]. The PMV was calculated based on averaged air temperature and humidity in the occupied zone for a seated person metabolic rate according to Fanger's standard expression for PMV in terms of environmental conditions, human typical clothing, and metabolic rate [25].

16

B. Model Validation Results

The experimentally measured temperatures at different elevations in addition to the exhaust and average wall temperatures, and DV load were compared to the model predicted values by operating the DV system alone at various internal loads as shown in Table 1.

Table 1: Experimental and Model Predicted Values of the displacement ventilation system at qs=0.118 m3/s, Ts=22 °C and RHsupply=50 %

| | Space Load | | | | | |
| | 200 W | | 300 W | | 400 W | |
Temperature	Exp.	Model	Exp.	Model	Exp.	Model
$T_{room\ at\ 0.5m}$ (ºC)	22.89±0.5	22.70	23.41±0.5	23.08	23.90±0.5	23.60
$T_{room\ at\ 1.1m}$ (ºC)	23.29±0.5	23.21	23.90±0.5	23.80	24.58±0.5	24.40
$T_{room\ at\ 2m}$ (ºC)	23.33±0.5	23.27	24.11±0.5	23.95	24.82±0.5	24.62
$T_{exhaust}$ (ºC)	23.39±0.5	23.34	24.16±0.5	24.03	24.91±0.5	24.70
$T_{wall\ avrg.}$ (ºC)	23.01±0.5	22.80	23.39±0.5	23.31	24.21±0.5	23.88

Load	(W)	206 ± 10	200	306 ± 10	300	412 ± 10	400

At the fixed supply conditions of q_s=0.118 m³/s, T_s=22 °C and *RH*=50 %, the highest internal loads were associated with the highest temperatures inside the space. Increasing the internal load from 200 W to 400 W caused a maximum increase in the temperature of air at the occupied level of 1.1 m by 1.29 °C experimentally and 1.19 °C by simulation. Also, the room air temperature was increasing vertically as it approaches the ceiling level, where it increased from 23.90 °C ± 0.5 to 24.91°C ± 0.5°C at internal load of 400 W. Thus, the PMV values for the different internal loads were estimated and found to be 0.19 ± 0.01, 0.31 ± 0.01 and 0.49 ± 0.01 at 200 W, 300 W and 400 W, respectively. In order to find the DV system load, the following equation is used:

$$Q_{DV} = \dot{m}C_p(T_{exhaust} - T_{supply}) \tag{11}$$

Where $\dot{m}$ is the supply air mass flow rate, C_p is the air specific capacity, $T_{exhaust}$ is the temperature of air leaving the space and T_{supply} is the supply air temperature.

Moreover, at different internal loads, good agreement was observed between measured experimental data and model predicted ones, so that the maximum error obtained was about 4% and 8% in the temperature readings and load calculation respectively.

As for the integrated DV/ECC system, the experimental measured temperatures at different elevations in addition to the ceiling and average wall temperatures, total load, and ECC load values obtained were compared to the model predicted ones

operating at various internal loads as shown in Table 2. At the fixed supply conditions of q_s=0.118 m^3/s, T_s=22 °C and RH=50 %, the highest internal loads were also associated with the highest temperatures of air at different elevations and ceiling and average wall temperatures, where the increase in the internal load from 200 to 400 W caused a maximum increase in the temperature of air at the occupied level of 1.1 m by 1.36 °C experimentally and 1.37 °C by simulation. Also, it was noticed that the room vertical temperature variation increased until the height of 1.1 m, where it reached a maximum of 24.52 °C ± 0.5°C experimentally at internal load of 400 W. The room temperature at the occupied level after that started to decrease as air approached the cooled ceiling, where the ceiling temperature reached values of 18.90°C ± 0.5°C, 19.32 °C ± 0.5°C and 19.70 °C ± 0.5°C at 200 W, 300 W and 400 W, respectively.

Table 2: Experimental and model predicted values of the integrated system at qs=0.118 m3/s, Ts=22 °C and RHsupply=50 %

| Temperature | Space Load | | | | | |
| | 200 W | | 300 W | | 400 W | |
	Exp.	Model	Exp.	Model	Exp.	Model
$T_{room\ at\ 0.5m}$ (°C)	22.65±0.5	22.45	23.00±0.5	22.82	23.64±0.5	23.20

$T_{room\ at\ 1.1m}$ (^{o}C)	23.16±0.5	23.01	23.86±0.5	23.68	24.52±0.5	24.38
$T_{room\ at\ 2m}$ (^{o}C)	23.01±0.5	22.80	23.64±0.5	23.45	24.42±0.5	24.23
$T_{ceiling\ inlet}$ (^{o}C)	22.20±0.5	22.16	22.76±0.5	22.70	23.45±0.5	23.36
$T_{ceiling}$ (^{o}C)	18.90±0.5	18.40	19.32±0.5	18.83	19.70±0.5	19.20
$T_{wall\ avrg.}$ (^{o}C)	21.40±0.5	21.25	21.85±0.5	21.60	22.32±0.5	22.10
Total Load (W)	202.0±12	200	305.50±12	300.0	408±12	400.0
ECC Load (W)	172.50±7	176.20	215.82±7	217.40	237±7	240.0

The increase in the internal load was associated with an increase in the PMV values that were found to be 0.02 ± 0.01, 0.16 ± 0.01 and 0.3 ± 0.01 at 200 W, 300 W and 400 W, respectively. These PMV values were lower than the ones obtained under the DV system, so that comfort in the space is enhanced.

The integrated DV/ECC system load is the summation of the DV and the ECC load represented by the convective heat exchange between the ceiling and its adjacent air layer and the radiative heat exchange between the ceiling and the walls of the space, according to the following equation:

$$Q_{DV/ECC} = Q_{DV} + h_c A(T_c - T_{air}) + h_r A(T_c - T_{MRT}) \tag{12}$$

where h_c is the convective heat transfer coefficient, A is the ceiling area, T_c is the average ceiling temperature, T_{air} is the air layer temperature adjacent to the ceiling, h_r is the linearized radiative heat transfer coefficient, and T_{MRT} is the mean radiant temperature of the walls.

The portion of the sensible load removed by the ECC was 176.2 W of the total load of 200 W representing 85.4% of the total sensible load. When the load was increased to 400 W, the ECC removed 240 W representing 58% of the room total sensible load. At low thermal load, the ECC is capable of removing most of the load from the space. At high load, the ECC system at T_c = 19.7 °C had larger temperature difference between supply air at 22 °C and ceiling adjacent air at 23.45 °C compared to the 200 W load and hence resulting in higher portion of the load to be removed by the DV system

Moreover, at different internal loads, good agreement was observed between measured experimental data and DV/ECC model predicted ones, so that the maximum error obtained was about 6% and 7% in the temperature readings and load removal calculation respectively.

C. Parametric Study

The parametric study aims to investigate the factors that affect the performance of the integrated system, mainly the supply flow rate and relative humidity parameters. The space considered for the parametric study is a 2.8 m × 2.8 m × 2.8 m space, and all walls were taken as internal partitions. Simulations were performed by taking constant internal load of 40 W/m², fixing the supply temperature to 21 ℃, and then increasing

first the supply air relative humidity from 10% to 90% at three supply air flow rate from 0.08 m^3/s to 0.2 m^3/s.

The variation of air temperature in the occupied zone and ceiling temperature are shown in Fig. 5 as a function of supply air relative humidity at supply flow rates of (a) 0.08 m^3/s, (b) 0.14 m^3/s and (c) 0.2 m^3/s. Figure 6 shows the DV and ECC loads as a function of supply air relative humidities at supply flow rates of (a) 0.08 m^3/s, (b) 0.14 m^3/s and (c) 0.2 m^3/s. For a given flow rate, the DV load increases with increased supply relative humidity (see Fig.6) since the temperature difference between the supply and exhaust air increases as observed in corresponding plots in Fig. 5 at all flow rates. However, the ceiling load decreased, since the air entering the ceiling setup is more humid. For example, at the flow rate of 0.08 m^3/s, increasing the relative humidity from 10 to 90%, decreased the ceiling load by 73.3%, since the ceiling temperature increased by 32.6%.
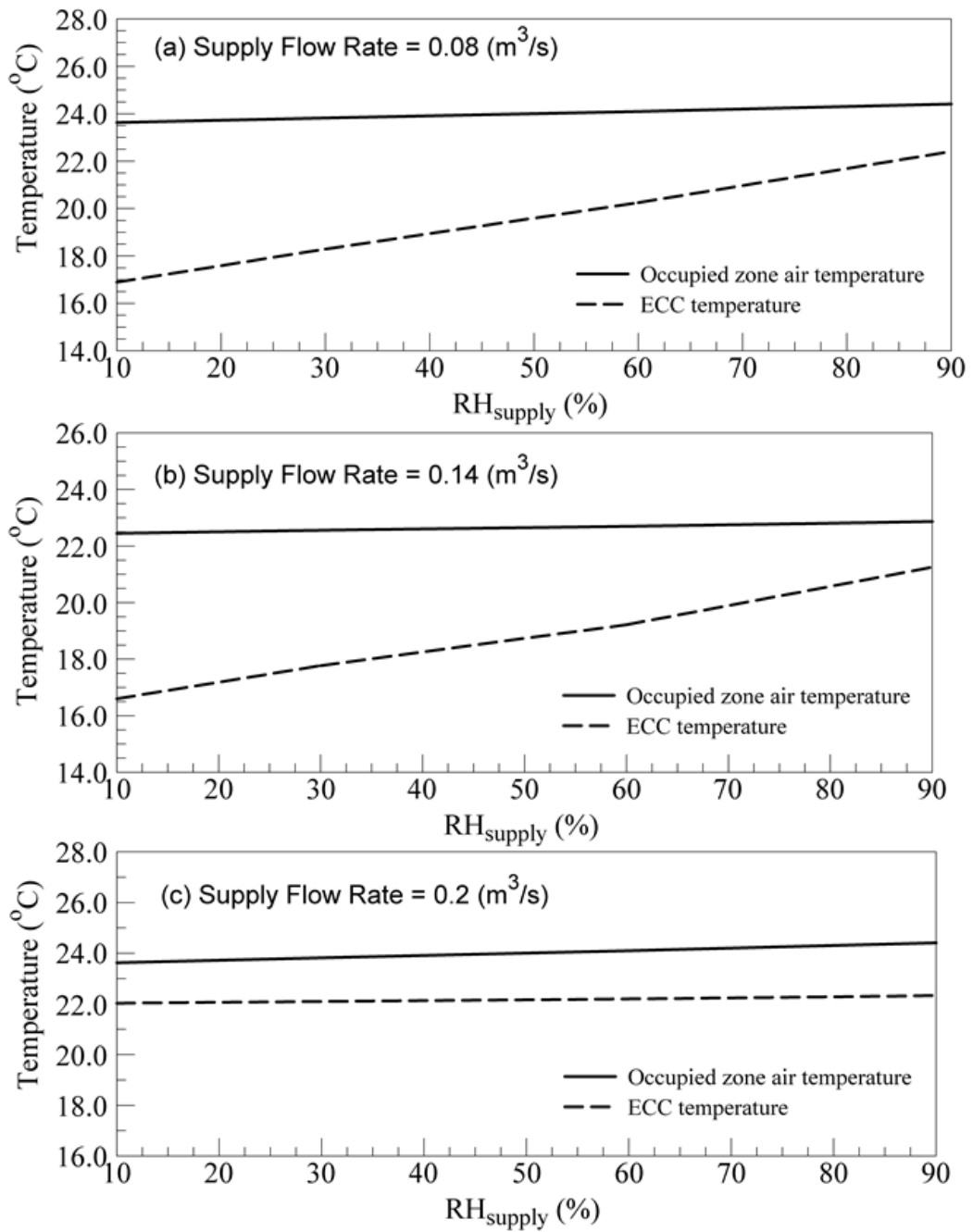
Figure 4: The variation of the temperatures of air in the occupied zone and ECC as a function of supply air relative humidity at supply flow rates of (a) 0.08 m3/s, (b) 0.14 m3/s and (c) 0.2 m3/s at fixed supply air temperature to 21 °

However, for a given supply relative humidity it is observed that when the supply flow rate is increased, the DV load decreased due to the decrease in the temperature difference between the supply and the exhaust air, while the cooled ceiling load increased, since the ceiling temperature decreases. At the supply relative humidity of 60%, increasing the flow rate from 0.08 m^3/s to 0.2 m^3/s increased the cooled ceiling load by 10.7% since the ceiling temperature decreased by 8.6% and the air temperature at the occupied level decreased by 7.9%. Therefore, the integrated system is proven to be more efficient at higher supply flow rates and lower supply relative humidity.
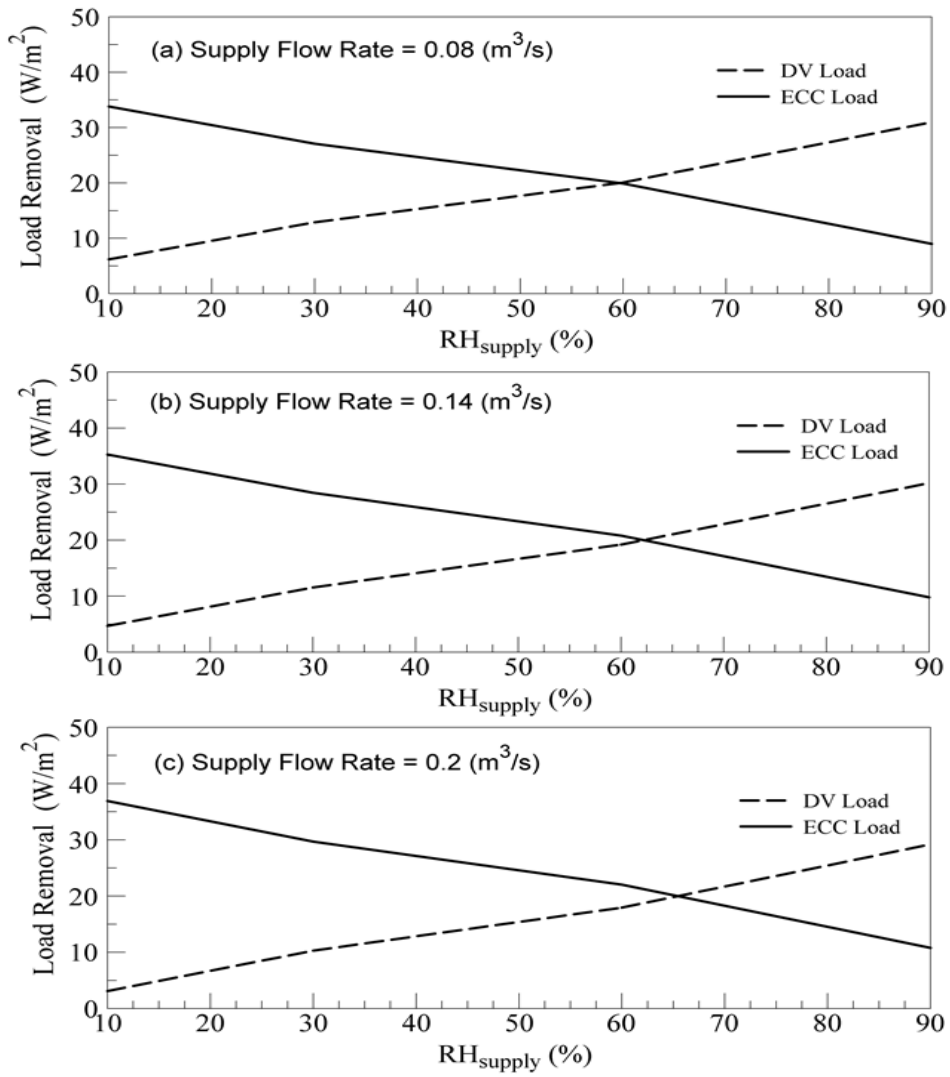
Figure 5: Plots of the DV and ECC loads as a function of supply air relative humidity at supply flow rates of (a) 0.08 m3/s, (b) 0.14 m3/s and (c) 0.2 m3/s at fixed supply air temperature to 21 ºC

CHAPTER IV

CASE STUDY

A. Case Study Description

The proposed integrated system is applied to a test case represented by an office space located in Beirut and simulated on a typical summer day of the cooling season during the occupied hours from 7 a.m. till 7 p.m. [26]. The integrated system electric consumption and operational cost are compared to those of a typical chilled ceiling and displacement ventilation (CC/DV) system operating under same conditions to derive the proposed system operational savings. The considered case for the study is a 6.0 m × 5.0 m × 2.8 m space as shown in Fig. 7, where the walls and floor are considered as internal partitions [27].
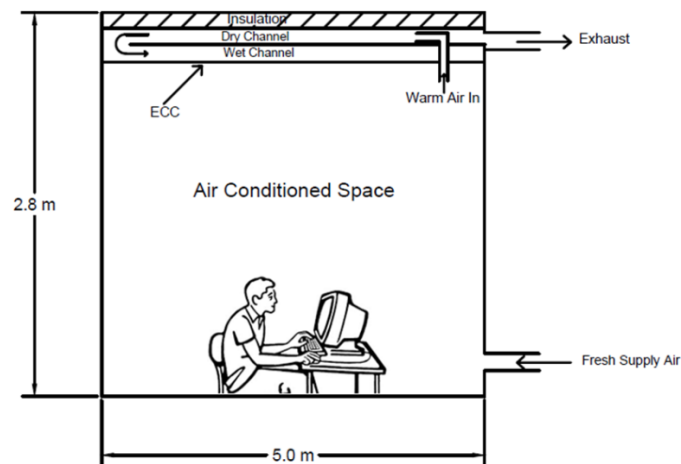

Figure 7: Schematic of the case study geometry and system used in the case study

Six occupants are present in the office according to the schedule shown in table 3. The sensible load per person is taken as 250 W, including lighting and equipment loads, and the moisture generation is 2×10^{-5} kg/s per occupant [7,21]. Table 4 also shows the internal sensible load during the different occupied hours. The load to be removed by the system is only due to internal heat sources and reaches values as high as 50 W/m^2, exceeding by that the limit the DV system can remove unaided (40 W/m^2). Therefore, after fixing the supply temperature and relative humidity to 20 ºC and 60 % respectively, a control strategy of increasing the supply flow rate is applied to the DV system, while maintaining the stratification height at 1.5 m, until reaching a limit where the DV system cannot maintain the comfort level anymore. The integrated system will thus be operated to improve the DV system performance.

B. Results and Discussion

Table 3 represents the variation of the results obtained upon operating the DV system alone. Between 7:00 a.m. and 9:00 a.m., the flow rate was set at 0.15 m^3/s. The internal load was around 17 W/m^2, so the DV system was able to remove this load while maintaining comfort in the space, with PMV values of 0, 0.02 and 0.03 at 7:00 a.m., 8:00 a.m. and 9:00 a.m., respectively. Upon increasing the internal load to 33.3 W/m^2 at noon, the flow rate was increased to 0.2 m^3/s, maintaining a stratification height of 1.5 m. The DV system was still able to provide comfort with a PMV value of 0.2 and acceptable temperatures at the occupied level of 23.68 ºC. However, during the peak load hours (13:00 p.m. to 15:00 p.m.) the internal load increased to 50 W/m^2, so the DV system under the control strategy applied was not able to maintain comfort in the space, with PMV values of 0.58, 0.61 and 0.64 at 13:00 p.m., 14:00 p.m. and 15:00 p.m.,

respectively. The air temperature at the occupied level increased significantly reaching 26.01 ℃; in addition to that, the ceiling temperature was high and reached a maximum of 23.09 ℃. Therefore, the integrated system will be operated to improve the performance of the DV system during peak load hours.

Upon operating the integrated system during the peak load hours (13:00 p.m. to 15:00 p.m.), it was noticed that the air temperature at the occupied level decreased to 24.31°C, 24.45 °C, and 24.57 °C, leading to PMV values of 0.39, 0.42 and 0.45 at 13:00, 14:00 and 15:00 p.m. respectively. Also, the ceiling temperature decreased to 19.72 °C, 20.29 °C and 20.31 °C at 13:00, 14:00 and 15:00 p.m. respectively. Therefore, comfort was attained during these peak hours after operating the integrated system, where the DV system was able to remove 50.6%, 52.5% and 53.4% of the internal load at 13:00, 14:00 and 15:00 p.m. respectively, and the remaining load was removed by the cooled ceiling.

Table 3: The variation of number of persons, supply flow rate, internal sensible load, air temperature, ceiling temperature, total load and PMV during occupied hours for a typical summer day

Occupied Hours	No of Persons	q_s (m³/s)	$Q_{internal}$ (W/m²)	T_{air} (℃)	$T_{ceiling}$ (℃)	Q (W/m²)	PMV DV	PMV DV/ECC
7	2	0.15	16.6	22.59	21.98	16.70	0	0
8	2	0.15	16.6	22.65	22.05	16.70	0.02	0.02
9	2	0.15	16.6	22.69	22.11	16.73	0.03	0.03

10	3	0.18	25.0	23.1	22.16	25.04	0.10	0.10
11	3	0.18	25.0	23.14	22.26	25.34	0.12	0.12
12	4	0.2	33.3	23.68	22.4	33.72	0.20	0.20
13	6	0.2	50.0	25.73	22.48	50.00	0.58	0.39
14	6	0.2	50.0	25.85	22.8	50.17	0.61	0.42
15	6	0.2	50.0	26.01	23.09	50.32	0.64	0.45
16	3	0.18	25.0	23.31	22.3	25.74	0.16	0.16
17	3	0.18	25.0	23.28	22.28	25.6	0.14	0.14
18	2	0.15	16.6	22.71	22.16	16.76	0.04	0.04
19	2	0.15	16.6	22.63	22.03	16.7	0.02	0.02

In order to find the electric power and cost savings of the proposed integrated system, a comparison with a typical CC/DV system was done. The operating electric power consumption is to be compared during the peak hours (13:00 p.m. to 15:00 p.m.) over the cooling season from June to October. Since the load to be removed is only due to internal loads and the same schedule is applied over the months of the cooling season, the same savings are expected to be obtained monthly. Therefore, the savings for one month are calculated and then multiplied by the number of months of the cooling season by estimating the chiller's operational power consumption. The COP of the chiller was taken to be 3.5, and the electrical cost was estimated at 0.15$/KWh.

Under the same operating conditions of the proposed case, but by using the CC/DV system at peak hours, the electric power consumption is found to be 477.62 kWh with a cost of $71.64 over the cooling season. While using the proposed integrated system, the power consumption was found to be 304.61 kWh with a cost of $45.69 over the same cooling period. Therefore, saving of 36.2 % was achieved over the cooling season where the reduction in electric energy consumption was 173.01 kWh and the corresponding reduction in operation cost was $25.95 during the cooling season.

C. Conclusion

A performance evaluation for an integrated displacement ventilation and evaporative cooled ceiling system is developed in order to enhance the cooling ability of the DV system. Mathematical models were developed and validated experimentally, where good agreement was found between modelled and experimental values.

A parametric study was also done in order to study the limitations of the system, where the DV/ECC showed better performance at higher supply flow rates and lower supply air relative humidity. The DV/ECC system extended the load removal range to values higher than the maximum value $40W/m^2$ that can be removed by DV system alone.

The integrated system was applied to a typical office space in the city of Beirut, where the electric power consumption is compared with that of a traditional chilled ceiling and displacement ventilation system operating under same conditions. The use of the proposed integrated system was shown to be effective with electric power savings exceeding 36% compared to conventional CC/DV system for the considered case of 50 W/m^2 load and for outdoor humidity at 60% and supply

temperature of 20°C. Clearly, the DV/ECC system would be recommended for

moderate climates with relative humidity lower than 60% to be effective.

BIBLIOGRAPHY

[1] DOE, Department of Energy, Information on the Commercial Buildings Sector, Energy Consumption by End Use for 1995, http://www.eia.doe.gov, 2001.

[2] Kharseh M, Altorkmany L, Al-Khawaj M, Hassani F. Warming impact on energy use of HVAC system in buildings of different thermal qualities and in different climates. Energy Convers Manage 2014;81:106–111.

[3] Vakiloroaya V, Samali B, Fakhar A, Pishghadam K. A review of different strategies for HVAC energy saving. Energy Convers Manage 2014;77:738–754.

[4] Gao CF, Lee WL, Chen H. Locating room air-conditioners at floor level for energy saving in residential buildings. Energy Convers Manage 2009;50: 2009–2019.

[5] Bjørn E, Nielsen PV. Dispersal of exhaled air and personal exposure in displacement ventilated rooms. Indoor Air 2002;12:147–164.

[6] Yuan X, Chen Q, Glicksman LR. A critical review of displacement ventilation. Energy and Building, ASHRAE Transaction. 1998; 104(1A):78–90.

[7] ASHRAE Handbook - Fundamentals Chapter 9. American Society of Heating Refrigerating and Air-Conditioning Engineers, Atlanta, 2009.

[8] Keblawi A, Ghaddar N, Ghali K, Jensen L. Chilled ceiling displacement ventilation design charts correlations to employ in optimized system operation for feasible load ranges. Energy Build 2009;41:1155–64.

[9] Rees SJ, Haves P. A nodal model for displacement ventilation and chilled ceiling systems in office spaces. Building and Environment 2001;36(6): 753–762

[10] Behne M. Indoor air quality in rooms with cooled ceilings: mixing ventilation or rather displacement ventilation? Energy Build 1999;30(2):155–66.

[11] Diaz NF. Experimental study of hydronic panels system and its environment. Energy Conversion and Management 2011;52(1):770–80.

[12] Ardehali MM, Panah NG, Smith TF. Proof of concept modeling of energy transfer mechanisms for radiant conditioning panels. Energy Conversion and Management 2004;45(13–14):2005–2017.

[13] Novoselac A, Srebric J. A critical review on the performance and design of combined cooled ceiling and displacement ventilation systems. Energy and buildings 2002; 34:497-509.

[14] Othamani M, Ghali K, Ghaddar N. Transient thermal comfort performance of radiant and convective heating system during startup period. November 17-19, 2008; The 4th International Conference on Energy research and Development (ICERD - 4), Kuwait.

[15] El Hourani M, Ghali K, Ghaddar N. Effective desiccant dehumidification system with two-stage evaporative cooling for hot and humid climates. Energy and Buildings 2014;68;329–338.

[16] Chakroun W, Ghaddar N, Ghali K. Chilled ceiling and displacement ventilation aided with personalized evaporative cooler. Energy and Buildings 43 (2011), 3250-3257.

[17] Hasan A. Indirect evaporative cooling of air to a sub-wet bulb temperature. Applied Thermal Engineering 2010;30(16):2460-2468

[18] Riangvilaikul B, Kumar RS. An experimental study of a novel dew point evaporative cooling system. Energy and Buildings 2010; 42:637–644.

[19] Miyazaki T, Akisawa A, Nikai I. Study on the Maisotsenko cycle evaporative cooler driven by the solar chimney. Proceedings of the 2010 Renewable Energy

Conference, Pacifica Yokohama, Japan, 27 June - 2 July 2010, Paper No O-Th-2-4, 2010.

[20] Kanaan M, Ghaddar N, Ghali K. Simplified model of contaminant dispersion in rooms conditioned by chilled ceiling displacement ventilation system. HVAC&R Res 2010;16:765–83.

[21] Ayoub M, Ghaddar N, Ghali K. Simplified thermal model of spaces cooled with combined chilled ceiling and displacement ventilation system. HVAC & R Res 2006;12:1005–30.

[22] Mundt E. The performance of displacement ventilation system, Ph. D thesis. Sweden: Royal Institute of Technology; 1996.

[23] Jaluria, Y. Natural Convection, Heat and Mass Transfer. Chapter 4. New York: Pergamon Press; 1980.

[24] Kanaan M, Ghaddar N, Ghali K, Araj G. New airborne pathogen transport model for upper-room UVGI spaces conditioned by chilled ceiling and mixed displacement ventilation: Enhancing air quality and energy performance. Energy Conversion and Management 2014;85,50–61.

[25] Fanger PO. Thermal Comfort Analysis and Applications in Engineering. New York: McGraw Hill, 1982.

[26] Ghaddar N, Bsat A. Energy conservation of residential buildings in Beirut. Int J Energy Res 1998;32(2):523–46.

[27] Yassine B, Ghali K, Ghaddar N, Srour I, Chehab G. A numerical modeling approach to evaluate energy-efficient mechanical ventilation strategies. Energy and Buildings 2012;55:618–63.